J. Applied Membrane Science & Technology, Vol. 30, August 2026, 231-246

Development of Wood Ash-Derived Geopolymer for Adsorptive Removal of Copper from Aqueous Solution

A. Nagesh[1], S. Mansur[1]*, M. N. Z. Abidin[2], M. S. C. Zain[1]

[1] Bioresource Technology Division, School of Industrial Technology, Universiti Sains Malaysia, Penang 11800, Malaysia.
[2] Department of Chemistry, Faculty of Science, Universiti Malaya, 50603 Kuala Lumpur, Malaysia

Submitted: 07/07/2026. Revised edition: 01/08/2026. Accepted: 01/08/2026. Available online: 21/08/2026

ABSTRACT

Heavy metal contamination by copper poses significant environmental risks, necessitating efficient and sustainable treatment technologies. This study investigated the potential of wood ash-derived geopolymer as a low-cost adsorbent for Cu^{2+} removal from aqueous solutions. Wood ash (WA) obtained from Acacia mangium was alkali-activated with metakaolin (MK) to synthesise a wood ash–metakaolin geopolymer (WAMK). The materials were characterised using particle size analysis (PSA), Fourier transform infrared spectroscopy (FTIR), and scanning electron microscopy coupled with energy-dispersive X-ray spectroscopy (SEM-EDX). Batch adsorption experiments were conducted under different pH conditions to evaluate Cu^{2+} removal performance. PSA showed that WAMK possessed the smallest particle size (D(0.9) = 42.87 μm) compared with WA (70.19 μm) and MK (48.10 μm), indicating improved particle refinement following geopolymerisation. WAMK successfully formed a stable aluminosilicate geopolymer structure, as confirmed by FTIR and SEM-EDX analyses. Under acidic conditions (pH 5), WA exhibited the highest Cu^{2+} removal efficiency (101.38%), whereas WAMK and MK achieved removal efficiencies of 40.09% and 18.71%, respectively. At pH 10, all adsorbents exhibited adsorption capacities ranging from 6.52 to 6.74 mg g^{-1} and 100% removal efficiencies, indicated that copper removal was influenced by both adsorption and $Cu(OH)_2$ precipitation under alkaline conditions. These findings demonstrate that solution pH plays a critical role in copper removal performance and that geopolymerisation successfully produced a structurally stable adsorbent with potential for sustainable wastewater treatment applications.

Keywords: Wood ash, geopolymer, adsorption, copper removal method, pH

1.0 INTRODUCTION

Copper is a heavy metal widely used in consumer products, industrial manufacturing, military applications, maritime activities, transportation, aerospace, and architectural materials. Despite its extensive applications, copper is also recognised as a persistent environmental pollutant that can accumulate in aquatic ecosystems and pose serious risks

* Corresponding to: S. Mansur (email: sumarni90@usm.my)
DOI: https://doi.org/10.11113/jamst.v30n2.354

to human health and the environment [1]. According to the National Academies Press (US) (2000), excessive copper exposure may cause acute mucosal irritation, gastrointestinal distress, kidney and liver damage, capillary injury, and central nervous system irritation [2]. Consequently, the effective removal of copper ions from wastewater has become an important environmental and public health concern.

Various technologies have been developed for the removal of copper from aqueous solutions, including chemical precipitation, membrane filtration, electrochemical treatment, biological treatment, and hydrogel-based processes [3–5]. However, these methods often suffer from several limitations, such as high operational and energy costs, excessive chemical consumption, complicated treatment procedures, incomplete metal removal, and the generation of large volumes of sludge [4]. Among the available treatment methods, adsorption has emerged as one of the most effective and widely applied techniques for heavy metal removal because of its high efficiency, operational simplicity, rapid response, low cost, and mild operating conditions [7]. In addition, adsorption technologies can use a wide variety of low-cost and waste-derived adsorbents, making them attractive for sustainable wastewater treatment applications.

Recent studies have demonstrated the potential of industrial and agricultural wastes as adsorbent materials for heavy metal remediation. Materials such as fly ash, wood ash, lignite, zeolite, red mud, rice husk ash, sawdust, chitosan, sugarcane bagasse, coconut shell, orange peel, and tea waste have shown promising performance in removing heavy metals from wastewater [8]. Among these materials, wood ash has gained attention because of its low cost, wide availability, and high mineral content [9]. Nevertheless, untreated wood ash is generally considered an inefficient direct adsorbent for copper ions. Its high alkalinity tends to increase the pH of aqueous solutions, promoting the precipitation of metal hydroxides rather than true adsorption processes [10]. Furthermore, wood ash possesses a relatively low surface area and lacks sufficient active functional groups compared with engineered adsorbents such as activated carbon and biochar, which limits its adsorption capacity for Cu^{2+} ions [11].

To overcome these limitations, the conversion of wood ash into geopolymer materials has emerged as a promising approach. Geopolymers are inorganic aluminosilicate materials synthesised through the alkali activation of silica- and alumina-rich precursors. They possess a highly porous three-dimensional network structure with negatively charged frameworks that can effectively immobilise cationic heavy metals through adsorption and ion-exchange mechanisms [12]. In addition, geopolymers exhibit high surface area, significant pore volume, and mesoporosity ranging from approximately 10 to 50 nm, all of which enhance the diffusion and retention of heavy metal ions within the adsorbent structure. Recent studies have reported the successful application of geopolymer-based adsorbents for copper removal from aqueous media due to their strong adsorption capacity, structural stability, and environmental sustainability.

Among the factors affecting copper adsorption, solution pH plays a critical role in determining adsorption efficiency. At low pH values, excess hydronium ions (H_3O^+) compete with Cu^{2+} ions for available adsorption sites, thereby reducing copper uptake. As the pH increases, the concentration of hydronium ions decreases, allowing greater interaction between Cu^{2+} ions and the negatively charged geopolymer surface. However, excessively high pH conditions can lead to the precipitation of copper hydroxide, $Cu(OH)_2$, reducing the concentration of free copper ions available for adsorption [13] Previous

* Corresponding to: S. Mansur (email: sumarni90@usm.my)
DOI: https://doi.org/10.11113/jamst.v30n2.354

studies have shown that the optimal pH for Cu^{2+} adsorption using metakaolin-based geopolymers is approximately pH 5, where adsorption is maximised while precipitation remains minimal [14].

Therefore, the development of wood ash-derived geopolymers represents a sustainable and cost-effective strategy for copper removal from aqueous solutions. By transforming waste wood ash into a functional geopolymer adsorbent, this approach not only enhances heavy metal adsorption performance but also promotes waste valorisation and environmental sustainability. The present study aims to investigate the potential of wood ash-derived geopolymers for the adsorption and removal of copper ions from aqueous solutions under controlled conditions.

2.0 EXPERIMENTAL

2.1 Materials

The *acacia mangium* species was chosen as the main material used in synthesising wood ash-derived geopolymer. The leftover wood chips of the *acacia mangium* species were collected from the wood laboratory of the Bioresource Technology Division, School of Industrial Technology, Universiti Sains Malaysia, as shown in Figure 1. Metakaolin was purchased from China. Both sodium hydroxide (NaOH) with a molecular weight of 40.0 g/mol and sodium silicate (Na_2SiO_3) with a molecular weight of 284.20 g/mol were purchased from R&M Chemicals, Malaysia, and Bendosen, Malaysia, respectively. Analytical grade copper (II) nitrate powder was obtained from Qrec, Malaysia. Hydrochloric acid was collected from laboratory 313 of the Bioresource Technology Division, School of Industrial Technology, Universiti Sains Malaysia (USM).

Figure 1. The leftover wood chips of *Acacia mangium sp*.

* Corresponding to: S. Mansur (email: sumarni90@usm.my)
DOI: https://doi.org/10.11113/jamst.v30n2.354

2.2 Preparation of Wood Ash-Derived Geopolymer

2.2.1 Preparation of Wood Ash

The collected wood chips underwent two stages of the grinding process. In the first stage, the wood chips were ground using a coarse grinder (Grinder Riken) with two different mesh sizes (3 and 2 mm). In the second stage, the pre-ground wood powder (WP) was further refined using a fine grinder (Grinder Retsch) equipped with a 1 mm mesh size. The ground WP was sieved using a sieve separator and filter machine (Tai-Yi Machine) fitted with a 100 µm mesh size. The sieved WP was subjected to carbonisation at 650 °C for 2 hours in a muffle furnace to form wood ash (WA). After cooling, the WA was ground using a pestle and mortar and sieved again with a mesh size of 75 µm to ensure uniform particle size. The final product was transferred into a dry container and stored in a desiccator for subsequent use in geopolymer synthesis.

2.2.2 Preparation of Alkaline Activator

The fabrication of the wood ash-derived geopolymer involved an alkali activation reaction between metakaolin and wood ash. A mixture of NaOH and Na_2SiO_3 was used as the alkaline activator. Initially, the alkaline activator solution was prepared by mixing 10 M of NaOH solution with Na_2SiO_3 solution in a 1:1 volume ratio. To prepare 50 mL of 10M NaOH solution, 20 g of NaOH pellets were carefully weighed and slowly dissolved in approximately 35–40 mL of distilled water in a heat-resistant beaker. The solution was stirred continuously until the pellets were completely dissolved and then allowed to cool to room temperature. Once cooled, the solution was diluted with additional distilled water to reach a final volume of 50 mL. Separately, 142.1 g of sodium silicate solution was measured to obtain an equivalent volume of 50 mL, based on its known density. The prepared 50 mL of NaOH solution and 50 mL of sodium silicate solution were then poured into a clean glass bottle and stirred using a magnetic stirrer at moderate speed until a uniform and homogeneous solution was obtained. The alkaline activator was then allowed to rest at room temperature for 24 hours to stabilise its chemical composition and viscosity before being used in the geopolymer synthesis process.

2.2.3 Synthesis of Wood Ash-Derived Geopolymer

The geopolymer paste for each geopolymer was prepared based on the composition shown in Table 1. A neat geopolymer without any addition of wood ash was labelled ‘MK’, while ‘WAMK’ represents a wood ash-derived geopolymer. Metakaolin was first mixed with WA prior to the addition of the alkaline activator to form a geopolymer paste.

Table 1. Neat and wood ash-derived geopolymer composition

Samples	Composition of the geopolymer		
	Wood ash (g)	Metakaolin (g)	Alkaline activator ($NaOH + Na_2SiO_3$) (g)
MK	0.0	10.0	10.0
WAMK	5.0	5.0	10.0

* Corresponding to: S. Mansur (email: sumarni90@usm.my)
DOI: https://doi.org/10.11113/jamst.v30n2.354

The prepared geopolymer paste was then cast into Petri dishes and placed in an oven for curing. The samples were cured at a constant temperature of 75°C for 24 hours, as shown in Figure 2. After cooling to room temperature, the neat and wood ash geopolymers were ground using a pestle and mortar. The ground samples were then sieved using a 75 µm mesh to achieve a uniform particle size. The final powders were stored in sealed glass bottles and placed in a desiccator for subsequent use in adsorption testing.

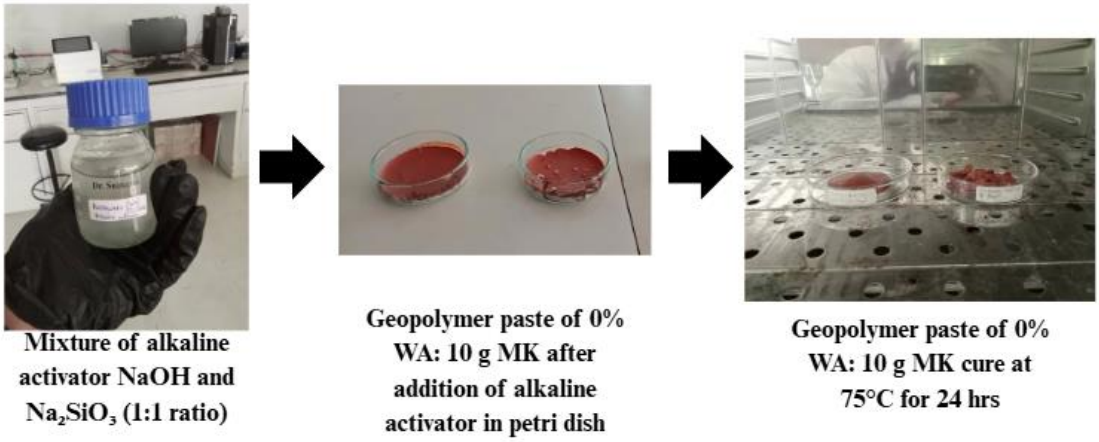

Figure 2. Summary of geopolymer fabrication

2.2.4 Characterisation of Wood Ash-Derived Geopolymer

The physical and chemical properties of the wood ash-derived geopolymers were analysed using particle size analysis (PSA), scanning electron microscopy with energy-dispersive X-ray spectroscopy (SEM-EDX), and Fourier-transform infrared spectroscopy (FTIR).

For PSA analysis, approximately 1–2 grams of the sample were dispersed in distilled water, which served as the dispersant. The suspension was subjected to ultrasonication for a few minutes to ensure uniform dispersion and to break apart any remaining clumps. The particle size measurement was performed under the "General Purpose" model setting, with the refractive index (RI) for the particles set at 1.520 and absorption at 0.1. The dispersant RI was set at 1.000 (water). The measurement range spanned 0.02 µm to 2000 µm, using enhanced sensitivity to capture fine and coarse particles.

SEM analysis was conducted to examine the surface morphology and microstructural features of the wood ash and the synthesised geopolymer samples. The powder samples were mounted onto carbon adhesive stubs, whereas WP and WA samples were coated with a thin layer of gold using a sputter coater to improve conductivity and prevent charging under the electron beam. SEM imaging was performed at magnifications of 500×, 2000×, and 10,000×. In conjunction with SEM analysis, EDX was performed to determine the elemental composition of the samples and to support the identification of chemical changes during geopolymer formation. EDX analysis was conducted on the same samples as WP, WA, MK and WAMK to detect and quantify major elements.

Finally, the FTIR spectra were recorded using an FTIR spectrometer in the range of 4000–400 cm^{-1} at a resolution of 4 cm^{-1}.

* Corresponding to: S. Mansur (email: sumarni90@usm.my)
DOI: https://doi.org/10.11113/jamst.v30n2.354

2.3 Geopolymer Adsorption Studies

The adsorption characteristics of WA, MK, and WAMK were determined by investigating the synthesised geopolymer under different solution pH conditions (pH 5, 7, and 10). This was done by gradually adding 0.1 M HCl to lower the pH or 0.1 M NaOH to increase it, while continuously stirring the solution. The pH of each solution was carefully monitored using a calibrated digital pH meter to ensure accuracy and prevent overshooting. Once the desired pH levels were achieved and stabilised, the solutions were used for batch adsorption tests to study the effect of pH on copper ion removal with various adsorbents.

For each adsorbent (WA, MK, and WAMK), 0.1 g of adsorbent dosage was tested in 10 mL of 60 ppm of copper (II) nitrate solution to evaluate the amount of copper adsorbed per gram of adsorbent. The solution was shaken using a mechanical shaker at 150 rpm for 24 hours to ensure uniform mixing and sufficient contact time between the adsorbent and the copper ions. All adsorption experiments were performed in triplicate to ensure the reliability and reproducibility of the results. After the 24 hours of the adsorption process, the mixtures were centrifuged at 4000 rpm for 10 minutes to separate the solid and liquid phases. The resulting supernatant was carefully collected and transferred into clean centrifuge tubes for subsequent analysis. The residual copper ion concentration in the supernatant was determined using Shimadzu Atomic Absorption Spectroscopy (AAS).

The adsorption capacity was determined using the following equation.

$$q_e = \frac{C_0 - C_e}{m} \times V \quad (1)$$

where q_e represents the adsorption capacity at equilibrium (mg/g), C_0 represents the initial concentration (mg/L), C_e represents the equilibrium concentration (mg/L), V represents the volume of solution (L), and m represents the mass of adsorbent (g).

The removal efficiency (R, %) of copper ions was calculated using the following equation:

$$R = \frac{C_0 - Ce}{C_0} \times 100 \quad (2)$$

where R is the removal efficiency, C_0 is the initial concentration of copper solution (mg/L), and C_e is the equilibrium concentration of copper solution (mg/L).

3.0 RESULTS AND DISCUSSION

3.1 Particle Size Analysis (PSA)

Table 2 presents the data on particle size distribution for WP, WA, MK, and WAMK. The parameter D(0.9) represents the particle diameter below which 90% of the sample volume is contained and is commonly used to indicate the presence of coarse particles within a material. Among all samples, WP exhibited the largest particle size, with a D(0.9) value of 305.70 µm, indicating a broad distribution of relatively coarse particles. This can be attributed to the fibrous and heterogeneous nature of raw wood powder, which still

* Corresponding to: S. Mansur (email: sumarni90@usm.my)
DOI: https://doi.org/10.11113/jamst.v30n2.354

contains significant amounts of cellulose, hemicellulose, and lignin. These organic constituents contribute to the larger and irregular particle morphology of untreated biomass materials [15]. The coarse structure also reflects the absence of thermal treatment, meaning the original architecture of the plant cell wall remained largely intact.

Following calcination, WA demonstrated a substantial reduction in particle size, with a D(0.9) value of 70.19 µm. The decrease in particle size is associated with the thermal decomposition of organic compounds during combustion, which removes volatile matter and converts the biomass into fine mineral-rich ash particles. According to Pitman (2006), the combustion process significantly alters the physical structure of wood-derived materials by producing finer and more porous ash residues [15]. The reduction in particle size observed for WA indicates that calcination effectively enhanced particle refinement and increased the availability of mineral phases suitable for geopolymer synthesis.

MK recorded a D(0.9) value of 48.10 µm, indicating a relatively fine and uniform particle distribution compared with WP and WA. The fine particle size of MK is attributed to its processed and calcined nature, which improves material homogeneity and increases specific surface area. Fine metakaolin particles are advantageous in geopolymer production because they enhance dissolution and reactivity during alkali activation. Genua *et al*. (2025) highlighted that the fineness of metakaolin plays a critical role in improving geopolymer consistency, mechanical performance, and reaction kinetics [16]. Therefore, the relatively small particle size of MK contributes positively to the formation of a more compact and reactive geopolymer matrix.

Among all samples, WAMK exhibited the finest particle size, with a D(0.9) value of 42.87 µm. The reduction in particle size following geopolymerisation suggests the formation of a more homogeneous and integrated aluminosilicate structure. The finer particle distribution of WAMK may also indicate improved particle packing and increased surface area, both of which are beneficial for adsorption applications. Smaller particles generally provide more accessible active sites and shorter diffusion pathways, thereby enhancing interaction between the adsorbent surface and metal ions in solution. This observation is consistent with the findings reported by Mosoarca *et al*. (2023), who noted that finer geopolymer particles contribute to improved adsorption performance due to enhanced surface characteristics and porosity [9].

Table 2. The particle size parameters for all samples

Sample	WP	WA	MK	WAMK
D(0.9) (µm)	305.70	70.19	48.10	42.87

Overall, the PSA results demonstrate that calcination and geopolymerisation significantly influence particle refinement and distribution. The progressive reduction in particle size from WP to WA, MK, and ultimately WAMK confirms that geopolymer formation enhances structural uniformity and produces finer particles with potentially higher surface area. These characteristics are important for environmental applications, particularly in heavy metal adsorption, as improved particle packing, increased porosity, and larger surface area can enhance adsorption efficiency and mass transfer properties.

* Corresponding to: S. Mansur (email: sumarni90@usm.my)
DOI: https://doi.org/10.11113/jamst.v30n2.354

3.2 Morphological Analysis

Figure 3 shows the SEM images of WP, WA, MK and WAMK at different magnifications.

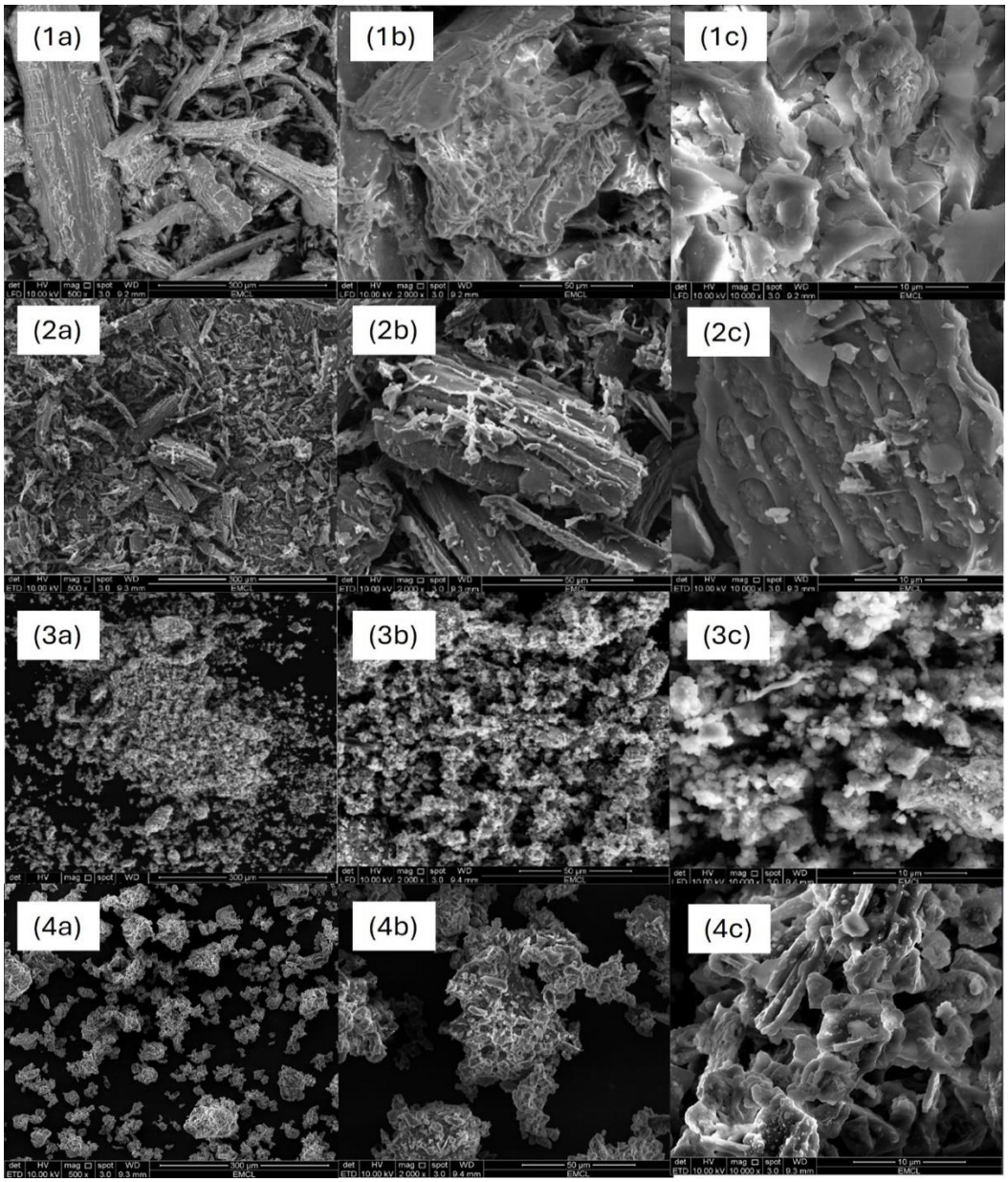

Figure 3. SEM images of (1) wood powder, (2) wood ash, (3) neat geopolymer, and (4) wood ash-derived geopolymer at different magnifications: (a) 500x, (b) 2000x, and (c) 10000x

Based on Figure 3(1a-c), the WP shows a fibrous, irregular structure with limited porosity and smooth surface features, typical of raw lignocellulosic material. After carbonisation, WA (Figure 3(2a-c)) has smaller particles and a rougher, more porous, and uneven surface than WP. Both neat geopolymers, MK and WAMK, exhibited aggregated,

* Corresponding to: S. Mansur (email: sumarni90@usm.my)
DOI: https://doi.org/10.11113/jamst.v30n2.354

more porous, and irregularly shaped particles. However, WAMK showed a larger apparent surface area than MK. The MK particles tended to agglomerate into dense clusters despite their highly porous structure, whereas the WAMK particles were more widely dispersed. This dispersion contributed to the increased surface area observed in WAMK. This observation is consistent with the PSA results, which showed that WAMK exhibits a smaller particle size than MK. Furthermore, at higher magnification (Figure 3(4c)), the WAMK particles appeared to be partially fused together, indicating the formation of interparticle bonding during geopolymerisation.

Table 3 indicates the percentage of elemental composition of WA, WP, MK, and WAMK. Prior to carbonisation, WP shows a high carbon (60.48 wt%) and oxygen (37.27 wt%) content, with only trace amounts of aluminum, Al (0.83 wt%), calcium, Ca (0.62 wt%), and sulphur, S (0.80 wt%). This composition reflects WP's organic nature and poor mineral content. WA demonstrated a dominant carbon content (84.26 wt%), which resulted from residual organic matter, as often seen in biomass ash [17].

The relatively high carbon signal observed for WA may be attributed to residual unburned carbon remaining after combustion, the heterogeneous distribution of carbon-rich regions within the ash, and the localised nature of SEM-EDX measurements. In addition, the use of carbon adhesive tape during sample preparation may have contributed to the detected carbon signal. Similar limitations of SEM-EDX in quantifying light elements such as carbon have been reported previously, and the technique is generally considered more suitable for qualitative or semi-quantitative surface elemental analysis than for determining bulk elemental composition[18].

The WAMK sample is mostly composed of silicon (7.70 wt%), aluminium (3.80 wt%), sodium (14.75 wt%), carbon (29.17 wt%), and oxygen (44.58 wt%). The predominance of oxide molecules, including SiO_2, Al_2O_3, and Na_2O, which are crucial components of the geopolymer network, is reflected in the high oxygen content [16]. According to Mosoarca *et al*. (2023), silicon and aluminium are the main structural components that form the amorphous aluminosilicate gel through Si–O–Al and Si–O–Si connections after alkali activation [9]. The introduction of sodium, by sodium silicate or NaOH, is essential for improving precursor dissolution and balancing the negative charge in the tetrahedral aluminosilicate structure [19]. Remaining unburned organic debris from the wood ash and carbonate phases, like $CaCO_3$ are responsible for the comparatively high carbon content [17]. Overall, the elemental distribution supports successful geopolymerisation and the formation of a stable alkali-activated matrix with potential uses in the copper adsorption process.

Table 3. EDX elemental composition of WA, WP, MK, and WAMK

Sample	Percentage weight of the element (%)						
	C	O	Al	S	Ca	Na	Si
WP	60.48	37.27	N/A	0.80	0.62	N/A	N/A
WA	84.26	14.03	N/A	N/A	N/A	1.71	N/A
MK	26.69	46.50	7.47	N/A	N/A	8.42	10.92
WAMK	29.17	44.58	3.80	N/A	N/A	14.75	7.70

* Corresponding to: S. Mansur (email: sumarni90@usm.my)
DOI: https://doi.org/10.11113/jamst.v30n2.354

3.3 FTIR Analysis

FTIR was used to determine the functional groups and chemical bonding properties of raw materials and geopolymer samples. The analysis was performed on WP, WA, MK, and WAMK to verify geopolymerisation and assess structural alterations. The FTIR graph in Figure 4 shows that WP has the common organic groups usually found in lignocellulosic biomass. The broad peak at 3337.08 cm^{-1} represents O-H stretching vibrations, typically caused by hydroxyl groups in cellulose and hemicellulose. The C–H stretching of the aliphatic -CH_2 and -CH_3 groups present in lignin is responsible for the peak at 2913.48 cm^{-1}. C–O stretching vibrations linked to ether linkages in hemicellulose and lignin structures are shown by a noticeable band at 1232 cm^{-1}. Finally, the C=C or Si–O–C stretching peak at 1030.41 cm^{-1} is more likely to be caused by polysaccharide backbones in this situation, particularly cellulose [15, 17]. These peaks confirm the presence of cellulose, hemicellulose, and lignin in the untreated wood powder before calcination.

Following calcination, WA showed a shift from organic to primarily inorganic functional groups. The breakdown of organic materials like cellulose and lignin after heat treatment is demonstrated by the elimination of O–H and C–H stretching bands. The existence of silicates and carbonates was confirmed by the appearance of new peaks, particularly at 1151.61 cm^{-1} (Si–O–Si or Si–O–Al stretching), 1568 cm^{-1} (asymmetric C=O or CO_3^{2-} stretching), 877 cm^{-1} (carbonate bending), and 749 cm^{-1} (Si–O bending). These results are in line with the research by Pitman (2006) and Barros *et al*. (2023), who found that because organic components are lost during burning, wood ash usually contains mineral phases like calcite and quartz [15, 17].

MK exhibited prominent inorganic functional groups, with strong peaks at 956.54 cm^{-1} (Si-OH or Al-O stretching) and 1447.60 cm^{-1} (carbonate bending), confirming the presence of reactive aluminosilicate structures. The full dehydroxylation and removal of organics during the calcination of kaolinite is further confirmed by the absence of organic-related peaks like O-H and C-H. Because of its reactive structure, MK is a perfect precursor to produce geopolymers, fostering the development of strong Si–O–Al frameworks that are necessary for binding and adsorption applications [9, 16].

WAMK exhibited significant peaks at 956.54 cm^{-1}, 1447.60 cm^{-1}, 836.67 cm^{-1}, and 680 cm^{-1}, showing the successful production of Si-O-Al and Al-O-Si bonds, which are typical for geopolymer compounds. Particularly noteworthy is the 836.67 cm^{-1} peak, which represents recently created Al–O–Si links connected to the hardened geopolymer framework [16]. The absence of organic residues from the wood ash and metakaolin is confirmed by the removal of large OH and CH peaks, indicating a full conversion into an inorganic matrix appropriate for environmental uses such as Cu^{2+} adsorption [9, 20].

* Corresponding to: S. Mansur (email: sumarni90@usm.my)
DOI: https://doi.org/10.11113/jamst.v30n2.354

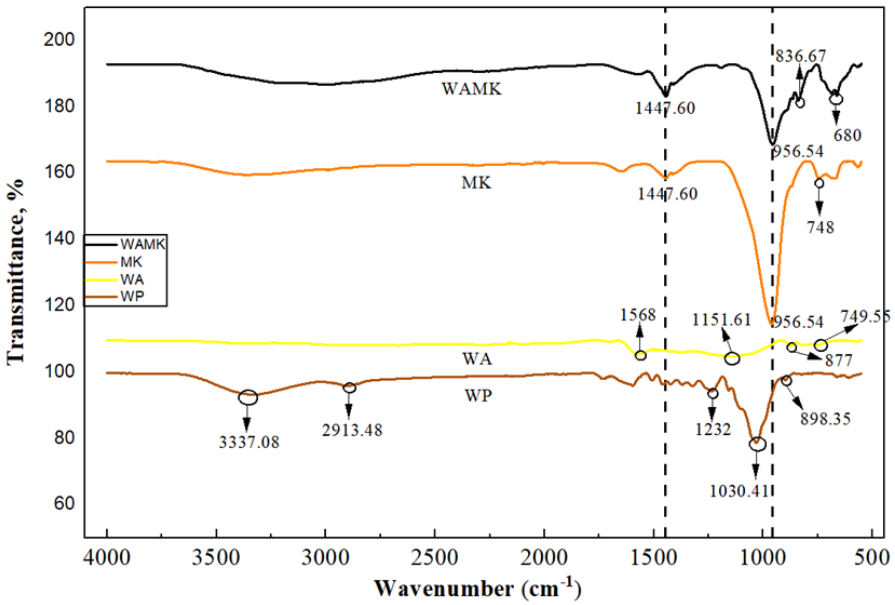

Figure 4. The FTIR Spectra of WP, WA, MK, and WAMK

3.4 Copper Adsorption Studies

As shown in Figure 5, all adsorbents exhibited a general trend in which the adsorption capacity decreased as adsorbent dosage increased. Although increasing the adsorbent dosage provides more available binding sites, the copper ion concentration remains constant, leading to underutilisation of active sites. This behaviour aligns with the findings of Satyam & Patra (2024), who reported that while overall removal efficiency may increase with higher dosage, the adsorption capacity per unit mass typically decreases [21].

At pH 10, the adsorption capacity curves for MK, WA, and WAMK intersected or closely converged at higher dosages, indicating that the differences in adsorption performance diminished as the system approached saturation. This trend was most apparent for MK, where Q_e dropped from 33.52 ± 0.00 mg/g at 0.02 g to 6.74 ± 0.00 mg/g at 0.10 g. The inverse relationship can be explained by the limited amount of copper ions available in the solution; as the dosage increases, more adsorption sites are introduced, but they remain underutilised due to site saturation and particle crowding, resulting in lower adsorption capacity per gram [21].

MK showed the highest Q_e across all dosages, suggesting a strong affinity for copper ions, possibly due to its high aluminosilicate content and greater surface reactivity. In comparison, WA recorded slightly lower Q_e values, with a decrease from 33.10 ± 0.00 mg/g to 6.66 ± 0.00 mg/g, consistent with its moderate porosity and mineral composition. WAMK, on the other hand, exhibited the lowest overall Q_e, ranging from 33.00 ± 0.00 mg/g to 6.52 ± 0.01 mg/g. These results confirm that while copper removal appears efficient at pH 10, the high Q_e values are partially influenced by chemical precipitation.

At pH 5, WA demonstrated the highest removal efficiency of 101.38%, indicating strong adsorption performance under mildly acidic conditions. This is consistent with WA's alkaline nature and porous surface structure, which enhances electrostatic interactions and ion exchange. In contrast, MK and WAMK showed a much lower percentage of removal,

* Corresponding to: S. Mansur (email: sumarni90@usm.my)
DOI: https://doi.org/10.11113/jamst.v30n2.354

with WAMK achieving a better removal efficiency of 40.09% compared to MK's 18.71%. The lower performance of MK at pH 5 may be attributed to competition between H^+ ions and Cu^{2+} for active sites, as discussed by Abbar *et al*. (2017) and Kumar *et al.* (2021) [22, 23].

At pH 7, the Q_e values for MK and WA increased to 6.52±0.01 mg/g and 6.20±0.01 mg/g, respectively, indicating enhanced adsorption due to reduced proton competition. However, WAMK exhibited a drop in Q_e to 1.05±0.03 mg/g and removal efficiency to 16.69%, suggesting possible surface passivation at this pH. MK showed an increase in percentage removal from 18.71% to 103.88%, potentially due to the onset of partial copper hydroxide precipitation, a phenomenon known to occur above pH 5. [16]. The negative adsorption capacity values that are observed for MK and WAMK is likely associated with the low affinity of the adsorbents for Cu^{2+} under these conditions, resulting in negligible adsorption.

At pH 10, all three adsorbents achieved high and nearly identical Q_e values, 6.74 ± 0.00 mg/g (MK), 6.66 ± 0.00 mg/g (WA), and 6.52 ± 0.01 mg/g (WAMK), alongside removal efficiencies exceeding 100%. These results suggest that the copper removal at this pH was influenced not only by adsorption but also by chemical precipitation of $Cu(OH)_2$, as supported by previous studies [7]. The convergence of Q_e values and the intersection of the line plots across adsorbents further indicate that precipitation dominated the removal mechanism, overshadowing the intrinsic differences in adsorbent properties.

In summary, WA demonstrated the most consistent performance across all pH levels, likely due to its moderate particle size, high alkalinity, and mineral content, as confirmed by PSA. MK showed significant improvement at higher pH, while WAMK displayed stability at pH 10 but poor performance under neutral conditions.

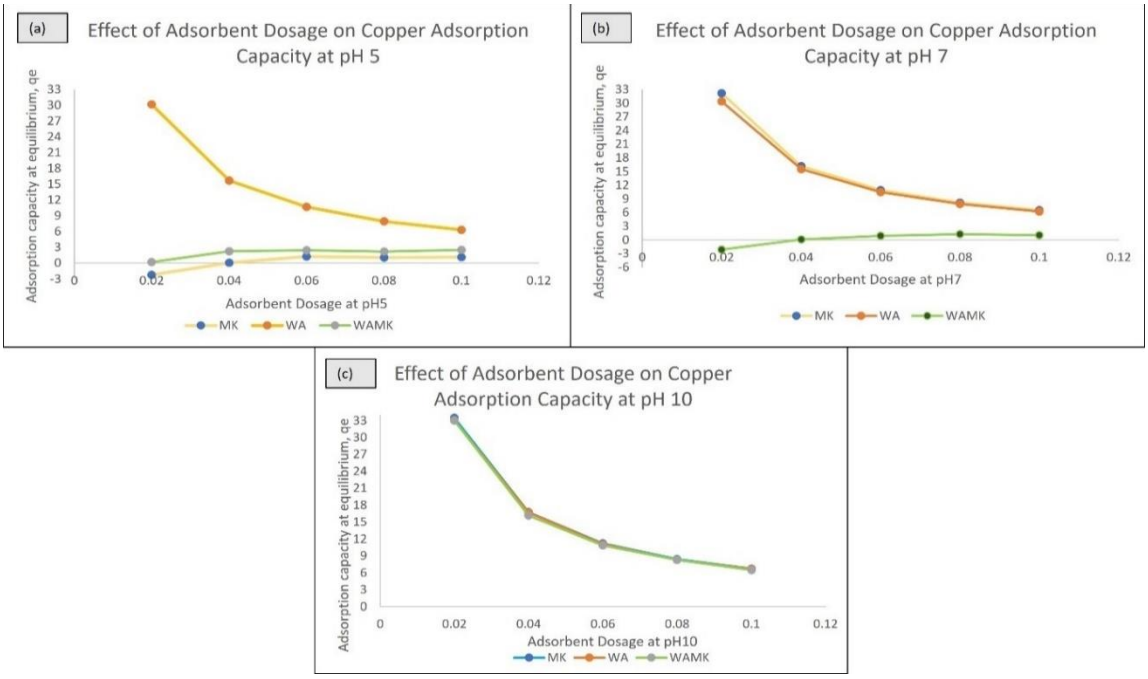

Figure 5. The effect of adsorbent dosage on copper adsorption capacity at (a) pH 5, (b) pH 7, and (c) pH 10 (error bars indicate standard deviations, n=3)

* Corresponding to: S. Mansur (email: sumarni90@usm.my)
DOI: https://doi.org/10.11113/jamst.v30n2.354

Based on Figure 6, the adsorption performance of the three adsorbents (MK, WA, and WAMK) is strongly influenced by solution pH. At pH 5, WA exhibited the highest removal efficiency (approximately 101.38%), whereas WAMK and MK achieved only 40.09% and 18.71%, respectively. The superior performance of WA may be attributed to the presence of mineral components, such as calcium-containing compounds and metal oxides, which can promote copper removal through surface complexation, ion exchange, and partial precipitation. In contrast, the adsorption capacities of MK and WAMK were reduced under acidic conditions because excess H_3O^+ ions competed with Cu^{2+} ions for the available adsorption sites, thereby limiting copper uptake.

When the solution pH was increased to pH 7, MK exhibited a marked increase in removal efficiency to approximately 103%, while WA maintained a high removal efficiency of approximately 98%. In contrast, WAMK showed a decrease in removal efficiency to 16.69%. This reduction suggests that geopolymerisation altered the availability of adsorption sites on WAMK, resulting in lower copper uptake under neutral conditions. The difference in behaviour between MK and WAMK indicates that incorporating wood ash into the geopolymer matrix modified the surface chemistry and adsorption characteristics of the material.

At pH 10, all adsorbents achieved removal efficiencies exceeding 100%. Under alkaline conditions, Cu^{2+} ions readily react with OH^- ions to form insoluble $Cu(OH)_2$, which substantially reduces the dissolved copper concentration. In addition to adsorption, the adsorbent surfaces may act as heterogeneous nucleation sites, facilitating the formation and deposition of $Cu(OH)_2$ precipitates. Consequently, copper removal at pH 10 resulted from the combined effects of adsorption and precipitation rather than adsorption alone. The removal efficiencies slightly exceeding 100% are likely due to experimental and analytical uncertainties associated with residual Cu^{2+} concentration measurements and should therefore be interpreted as indicating nearly complete copper removal rather than adsorption exceeding the theoretical maximum.

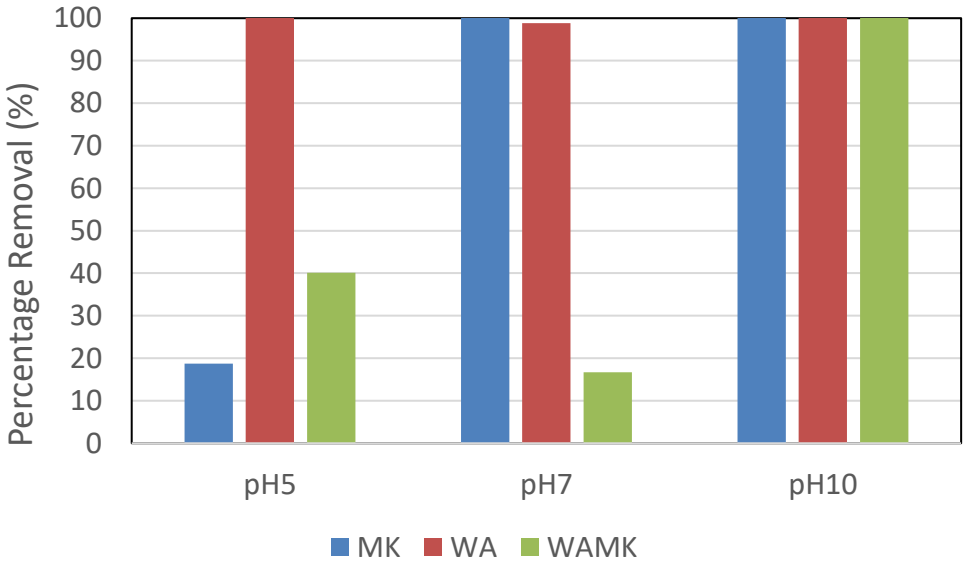

Figure 6. The percentage removal of 0.1 g adsorbent towards copper at different pH (error bars indicate standard deviations, n=3)

* Corresponding to: S. Mansur (email: sumarni90@usm.my)
DOI: https://doi.org/10.11113/jamst.v30n2.354

4.0 CONCLUSION

Wood ash-derived geopolymer (WAMK) was successfully synthesised via the alkali activation of wood ash and metakaolin. PSA, FTIR, and SEM-EDX results confirmed the formation of a stable aluminosilicate geopolymer structure with a finer particle size (D(0.9) = 42.87 μm) than WA (70.19 μm) and MK (48.10 μm). Adsorption performance was strongly influenced by solution pH. At pH 5, WA exhibited the highest Cu^{2+} removal efficiency (101.38%), while WAMK and MK achieved 40.09% and 18.71%, respectively. At pH 10, all adsorbents exhibited adsorption capacities ranging from 6.52 to 6.74 mg g^{-1}, although copper removal was influenced by the precipitation of $Cu(OH)_2$ under alkaline conditions. This confirms that the geopolymerisation process successfully created a well-structured material with potential for copper removal. The pH of the solution played an important role in adsorption performance. At low pH (5), the presence of excess H_3O^+ ions competed with copper ions for active sites, reducing adsorption. At high pH (10), copper ions began to form precipitates like Cu $(OH)_2$, making it difficult to measure true adsorption. Based on the data, pH 5 was identified as the optimal condition for copper adsorption without interference from precipitation. This study shows that wood ash-derived geopolymer is a promising, sustainable, and cost-effective material for removing copper ions from water. It offers improved performance through geopolymerisation and contributes useful knowledge for developing environmentally friendly solutions in wastewater treatment.

DECLARATION OF COMPETING INTEREST

The authors declare that they have no known competing financial interests or personal relationships that could have appeared to influence the work reported in this paper.

ACKNOWLEDGEMENT

The authors gratefully acknowledge the financial support given by Universiti Sains Malaysia through a Short-Term Grant (R501-LR-RND002-0000000908-0000) and the Kurita Water and Environment Foundation (R504-LR-GAL008-0000002071-K120).

REFERENCES

[1] Cui, L., Cheng, C., Li, X., Gao, X., Lv, X., Wang, Y., Zhang, H., & Lei, K. (2024). Comprehensive assessment of copper's effect on marine organisms under ocean acidification and warming in the 21st century. *Science of The Total Environment*, *927*, 172145. https://doi.org/10.1016/j.scitotenv.2024.172145

[2] Royer, A., & Sharman, T. (2026). *Copper Toxicity*. StatPearls Publishing.

[3] Sossou, K., Bala Prasad, S., & Segotsi, J. T. (2024). Removal of copper ions from aqueous solutions using a nanomembrane ceramic filter doped with magnetic zeolite. *Cleaner Water*, *2*, 100057. https://doi.org/10.1016/j.clwat.2024.100057

[4] Liu, Y., Wang, H., Cui, Y., & Chen, N. (2023). Removal of copper ions from wastewater: A review. *International Journal of Environmental Research and Public Health*, *20*(5), 3885. https://doi.org/10.3390/ijerph20053885

[5] Jeremias, J. S. D., Lin, J.-Y., Dalida, M. L. P., & Lu, M.-C. (2023). Abatement

* Corresponding to: S. Mansur (email: sumarni90@usm.my)
DOI: https://doi.org/10.11113/jamst.v30n2.354

technologies for copper containing industrial wastewater effluents – A review. *Journal of Environmental Chemical Engineering*, *11*(2), 109336. https://doi.org/10.1016/j.jece.2023.109336

[6] Qasem, N. A. A., Mohammed, R. H., & Lawal, D. U. (2021). Removal of heavy metal ions from wastewater: A comprehensive and critical review. *Npj Clean Water*, *4*(1), 36. https://doi.org/10.1038/s41545-021-00127-0

[7] Shrestha, R., Ban, S., Devkota, S., Sharma, S., Joshi, R., Tiwari, A. P., Kim, H. Y., & Joshi, M. K. (2021). Technological trends in heavy metals removal from industrial wastewater: A review. *Journal of Environmental Chemical Engineering*, *9*(4), 105688. https://doi.org/10.1016/j.jece.2021.105688

[8] Mosoarca, G., Vancea, C., Popa, S., Boran, S., Negrea, P., & Radulescu-Grad, M. E. (2023). STUDIES regarding copper ions removal from wastewaters using oak wood ash and the effect of exhausted ash as soil amendment. *Studia Universitatis Babeș-Bolyai Chemia*, 193–209. https://doi.org/10.24193/subbchem.2023.1.14

[9] Cairns, S., Chaudhuri, S., Sigmund, G., Robertson, I., Hawkins, N., Dunlop, T., & Hofmann, T. (2021). Wood ash amended biochar for the removal of lead, copper, zinc and cadmium from aqueous solution. *Environmental Technology & Innovation*, *24*, 101961. https://doi.org/10.1016/j.eti.2021.101961

[10] Wang, Y., Li, H., & Lin, S. (2022). Advances in the study of heavy metal adsorption from water and soil by modified biochar. *Water*, *14*(23), 3894. https://doi.org/10.3390/w14233894

[11] Arokiasamy, P., Abdullah, M. M. A. B., Abd Rahim, S. Z., Sadique, M., Ming, L. Y., Mohd Salleh, M. A. A., Mohd Arif Zainol, M. R. R., & Ghazali, C. M. R. (2023). Diverse material based geopolymer towards heavy metals removal: a review. *Journal of Materials Research and Technology*, *22*, 126–156. https://doi.org/10.1016/j.jmrt.2022.11.100

[12] Kara, I., Tunc, D., Sayin, F., & Akar, S. T. (2018). Study on the performance of metakaolin based geopolymer for Mn(II) and Co(II) removal. *Applied Clay Science*, *161*, 184–193. https://doi.org/10.1016/j.clay.2018.04.027

[13] Buema, G., Trifas, L.-M., & Harja, M. (2021). Removal of toxic copper ion from aqueous media by adsorption on fly ash-derived zeolites: Kinetic and equilibrium studies. *Polymers*, *13*(20), 3468. https://doi.org/10.3390/polym13203468

[14] Pitman, R. M. (2006). Wood ash use in forestry - A review of the environmental impacts. *Forestry*, *79*(5), 563–588. https://doi.org/10.1093/forestry/cpl041

[15] Genua, F., Lancellotti, I., & Leonelli, C. (2025). Geopolymer-based stabilization of heavy metals, the role of chemical agents in encapsulation and adsorption: Review. *Polymers*, *17*(5), 670. https://doi.org/10.3390/polym17050670

[16] Barros, D., Fernandes, É., Jesus, M., Barros, L., Alonso-Esteban, J. I., Pires, P., & Vaz Velho, M. (2023). The chemical characterisation of the maritime pine bark cultivated in Northern Portugal. *Plants*, *12*(23), 3940. https://doi.org/10.3390/plants12233940

[17] Goldstein, J. I., Newbury, D. E., Michael, J. R., Ritchie, N. W. M., Scott, J. H. J., & Joy, D. C. (2018). *Scanning Electron Microscopy and X-Ray Microanalysis*. Springer New York. https://doi.org/10.1007/978-1-4939-6676-9

[18] He, P., Xin, K., Zhang, X., Guo, Z., & Zheng, W. (2023). Development of an activated carbon-geopolymer composite for treatment of Pb(II) polluted water and

* Corresponding to: S. Mansur (email: sumarni90@usm.my)
DOI: https://doi.org/10.11113/jamst.v30n2.354

soil. *International Journal of Applied Ceramic Technology*, *20*(5), 3027–3040. https://doi.org/10.1111/ijac.14393

[19] Zahidah, Z., Sik, H., How, S., Ho, W., Ramzul Iklas, A., & Tanjong, A. (2023). Assessment of kiln dried acacia mangium for production of quality value-added products. *Journal of Tropical Forest Science*, *35*(Special Issue), 67–74. https://doi.org/10.26525/jtfs2023.35S.SI.67

[20] Satyam, S., & Patra, S. (2024). Innovations and challenges in adsorption-based wastewater remediation: A comprehensive review. *Heliyon*, *10*(9), e29573. https://doi.org/10.1016/j.heliyon.2024.e29573

[21] Abbar, B., Alem, A., Marcotte, S., Pantet, A., Ahfir, N.-D., Bizet, L., & Duriatti, D. (2017). Experimental investigation on removal of heavy metals (Cu2+, Pb2+, and Zn2+) from aqueous solution by flax fibres. *Process Safety and Environmental Protection*, *109*, 639–647. https://doi.org/10.1016/j.psep.2017.05.012

[22] Kumar, M., Seth, A., Singh, A. K., Rajput, M. S., & Sikandar, M. (2021). Remediation strategies for heavy metals contaminated ecosystem: A review. *Environmental and Sustainability Indicators*, *12*, 100155. https://doi.org/10.1016/j.indic.2021.100155

* Corresponding to: S. Mansur (email: sumarni90@usm.my)
DOI: https://doi.org/10.11113/jamst.v30n2.354